

Crossover between ballistic and diffusive regime of the spin-conductance and CPP-GMR in magnetic multilayered nanostructures

S. Sanvito*,

*School of Physics and Chemistry, Lancaster University, Lancaster, LA1 4YB, UK and
DERA, Electronics Sector, Malvern, Worcs. WR14 3PS UK*

C.J. Lambert†,

School of Physics and Chemistry, Lancaster University, Lancaster, LA1 4YB, UK

J.H. Jefferson,

DERA, Electronics Sector, Malvern, Worcs. WR14 3PS, UK

(February 26, 2018)

We analyze the interplay between disorder and band structure in current perpendicular to the planes (CPP) giant magnetoresistance (GMR). We consider finite magnetic multilayers attached to pure crystalline leads, described by a tight-binding simple cubic two-band model (s - d). Several models of disorder are considered, including random on-site potentials, lattice distortions, impurities, vacancies, and cross-section fluctuations. Magneto-transport properties are calculated in the zero-temperature zero-bias limit, within the Landauer-Büttiker formalism. Using a very efficient numerical scattering technique, we are able to perform simulations, over large length scales, and to investigate spin-transport in the ballistic, diffusive and localized regimes, as well as the crossover between them. The competition between disorder-induced mean free path reduction and disorder-induced spin asymmetry enhancement of the conductance highlights several different regimes of GMR.

PACS: 73.23-b, 75.70-i, 75.70Pa

I. INTRODUCTION

Spin filtering in transition metal magnetic multilayers, which arises when the magnetizations of adjacent layers switch from an anti-parallel (AP) to a parallel (P) alignment, is fundamental to the occurrence of giant magnetoresistance (GMR) [1,2]. The resistance in the anti-aligned state can be as much as 100% higher than the resistance with parallel alignment, leading to magnetic field sensors with sensitivity far beyond that of conventional anisotropic magnetoresistance (AMR) devices. In the most common experimental setup, the current flows in the plane of the layers (CIP), and the resistance is measured with conventional multi-probe techniques. Measurements in which the current flows perpendicular to the planes (CPP) are more delicate because the resistances involved are small. Despite this feature the use of superconducting contacts [3], sophisticated lithographic techniques to form multilayered pillar structures [4], and electrodeposition [5–7], makes such measurements possible and to date a large amount of experimental data has been produced (for recent reviews see references [8,9]). In the CPP configuration an electron propagates across the whole multilayered structure, while in the CIP configuration it can in principle traverse the system without being scattered at a ferromagnetic/normal metal interface. This makes the CPP configuration more effective at filtering the current and consequently CPP-GMR is generally larger than its CIP counterpart. In what follows we shall focus our attention solely on CPP GMR.

On the theoretical side two fundamentally different approaches have been used to describe CPP GMR. The first assumes that all the transport is diffusive and is based on the semi-classical Boltzmann equation within the relaxation time approximation. This model has been developed by Valert and Fert [10], and has the great advantage that the same formalism describes both CIP and CPP experiments. It identifies the characteristic lengths of the problem and can include the effects of disorder into the definition of the spin σ dependent mean free path λ_σ and spin the diffusion length l_{sf} . Moreover it can be extended to describe the temperature dependence of GMR [11]. In the limit that the spin diffusion length is much larger than the layer thicknesses (infinite spin diffusion length limit), this model

*e-mail: sanvito@dera.gov.uk

†e-mail: c.lambert@lancaster.ac.uk

reduces to a classical two current resistor network, in which additional spin-dependent scattering at the interfaces is considered. The resistor network model has been used since the early days of CPP GMR by the Michigan State University group [12], and describes most of the experimental data. The parameters of the model are the magnetic (non magnetic) metal resistivity ρ_M^* (ρ_N^*), the spin asymmetry parameter β introduced through the spin dependent resistivity of the magnetic metal $\rho_{\uparrow(\downarrow)} = 2\rho_M^*(1 - (+)\beta)$, the magnetic/normal metal interface resistance per unit area r_b^* and the interface scattering spin asymmetry γ introduced through the spin-dependent interface resistance per unit area $r_{\uparrow(\downarrow)} = 2r_b^*(1 - (+)\gamma)$. A good fit of the parameters has been shown to be possible, and the same value can fit reasonably well both the CIP and the CPP data [12]. The limitation of such a model is that it neglects the band structure of the system, and all the parameters are phenomenological. An extension of the model to include band structure has been made recently [13,14], implementing the above transport theory within the framework of density functional theory in the local spin density approximation. In this calculation, the scattering due to impurities is treated quantum mechanically, while transport is described semi-classically using the Boltzmann equation. Material dependent studies are possible, but the calculations are very computationally expensive and it is not possible to deal with disordered systems.

The second theoretical approach to CPP GMR is based on the quantum theory of scattering. Schep, Kelly, and Bauer [15,16] showed that band structure alone could account for the large CPP GMR found in Co/Cu multilayers. Their calculations are based on local density functional theory and the Sharvin resistance of a small constriction formed from a pure crystalline infinite superlattice is calculated. This approach is completely *ab-initio* but can deal only with clean systems, and the unit cell must be small. To perform *ab-initio* studies of phase coherent transport in disordered multilayers, more efficient numerical techniques are required. Tight-Binding methods based on *spd* Hamiltonians derived from first principle calculations have been employed by several groups [17–19]. On the one hand they can describe quite accurately the band structure of the transition metal multilayers, and on the other their computer overheads are more modest with respect to density functional calculations. As such they are suitable for numerical descriptions of long multilayers attached to realistic pure crystalline leads. Nevertheless the study of disorder using *spd* tight-binding models is not trivial, because the large number of degrees of freedom necessary to reproduce an accurate band structure leads quickly to unmanageably large matrices. The only calculations carried out to date involve either infinite superlattices in the diffusive regime [17] where small unit cells must be used, or finite superlattices in which disorder is introduced without breaking translational symmetry in the direction perpendicular to the current [18,20]. In the latter case the system is an effective quasi 1D system, whereas real multilayers are 3D systems with roughness at the interfaces which breaks translational invariance.

The aim of the present paper is to study three dimensional GMR multilayers and to investigate the effect of the disorder-induced cross-over between ballistic and diffusive transport. To address this problem we consider a reduced tight-binding model with two degrees of freedom (*s-d*) per atomic site. We use a technique already employed to describe pure crystalline structures [19] to compute the zero-bias zero-temperature conductance in the framework of the Landauer-Büttiker approach [21]. We have optimized the calculation such that it scales sub-linearly with the multilayer length. Several models of disorder are introduced in order to mimic defects, impurities, vacancies and lattice imperfections. In the case of multilayered nanowires [5–7] where the phase breaking length is comparable with the wire cross-section, we consider the effects of rough boundaries and confinement. We show that phase coherent transport in disordered magnetic multilayers may give rise to behavior not describable by the Boltzmann approach and discuss the relevance of these “non-diffusive” effects in several new experiments.

The paper is organized as follows: in section 2 we describe our implementation of a numerical scattering technique capable of handling large systems and performing efficient averages over large ensembles. We also discuss the *s-d* model which is the minimal Hamiltonian capable of capturing inter-band scattering. In section 3 we present the main results of this paper and discuss the effect of different sources of disorder and finally we conclude in section 4.

II. AN EFFICIENT NUMERICAL SCATTERING TECHNIQUE AND MODELS OF DISORDER

A. Numerical Technique and a two band Model

The numerical technique used in the present calculation has been outlined in reference [19], and describes an arbitrarily long finite multilayer attached to two crystalline semi-infinite leads. The spin-dependent conductance Γ^σ of such a structure is computed by evaluating the Landauer-Büttiker formula [21]

$$\Gamma^\sigma = \frac{e^2}{h} T^\sigma = \frac{e^2}{h} \sum_{k_\parallel}^{\text{BZ}} T^\sigma(k_\parallel), \quad (2.1)$$

where e is the electronic charge, h Planck's constant, and T^σ ($\sigma = \uparrow, \downarrow$) the total spin-dependent transmission coefficient, defined as $T^\sigma = \text{Tr } t^\sigma t^{\sigma\dagger}$ with t^σ the transmission matrix of the system. The second equality is valid in the case of translational invariance and the sum is taken over the 2D Brillouin zone in the direction orthogonal to the current. As a matter of notation we use the symbol \parallel to indicate k -points in the plane of the layers, and the symbol \perp to indicate the direction of the current. We completely neglect processes leading to spin mixing effects and the two spin currents are treated separately. To utilize this expression in the presence of disorder, we consider a disordered wire of finite cross-section, which is periodically repeated in the transverse direction. In the diffusive limit, this coincides with the infinite spin-diffusion length limit of the Valert and Fert theory which is equivalent to a classical resistor model. We define Γ_P^\uparrow (Γ_P^\downarrow) to be the conductance of the majority (minority) spins in the parallel alignment, and $\Gamma_{AP}^{\uparrow\downarrow}$ to be the conductance for both spins in the anti-parallel alignment, which yields for the GMR ratio,

$$\text{GMR} = \frac{\Gamma_P^\uparrow + \Gamma_P^\downarrow - 2\Gamma_{AP}^{\uparrow\downarrow}}{2\Gamma_{AP}^{\uparrow\downarrow}}. \quad (2.2)$$

The Hamiltonian for the whole system can be written

$$H = H_L + H_{LM} + H_M + H_{MR} + H_R, \quad (2.3)$$

with H_L (H_R) the Hamiltonian of the semi-infinite left- (right-) -hand lead, H_{LM} (H_{MR}) the coupling matrix between the left (right) lead and the multilayer, and H_M the Hamiltonian of the multilayer. The key point is that we can decouple the calculation of the scattering channels in the leads from the calculation of an effective Hamiltonian describing the multilayer. Consider first the retarded Green's function of the two decoupled semi-infinite leads

$$g(E) = (E - H_L - H_R + i0^+)^{-1}. \quad (2.4)$$

If the surface of the leads contains M atoms each described by n degrees of freedom, the Green's function g is a $(nM) \times (nM)$ matrix. Hence the surface Green's function g^S involving only degrees of freedom of the left and right lead surfaces is a $(2nM) \times (2nM)$ matrix whose matrix elements g_{ij}^S coupling the two leads vanish. The block-diagonal matrix g^S can be computed by evaluating the semi-analytic expression given in reference [19]. Such a semi-analytic expression is valid if the Hamiltonian describing a crystalline lead can be written in the following trigonal form

$$H = \begin{pmatrix} \dots & \dots & \dots & \dots & \dots & \dots & \dots & \dots \\ \dots & H_0 & H_1 & 0 & \dots & \dots & \dots & \dots \\ \dots & H_{-1} & H_0 & H_1 & 0 & \dots & \dots & \dots \\ \dots & 0 & H_{-1} & H_0 & H_1 & 0 & \dots & \dots \\ \dots & 0 & 0 & H_{-1} & H_0 & H_1 & 0 & \dots \\ \dots & \dots & \dots & \dots & \dots & \dots & \dots & \dots \\ \dots & \dots & \dots & \dots & \dots & \dots & \dots & \dots \end{pmatrix}, \quad (2.5)$$

where H_0 is an hermitian matrix describing the coupling within a cross-sectional slice of the lead, and H_1 ($H_{-1} = H_1^\dagger$) is the coupling matrix between adjacent slices. Once g^S is computed, the total surface Green's function G^S of the leads + multilayer can be calculated by solving Dyson's equation

$$G^S(E) = [(g^S(E))^{-1} - \tilde{H}_M]^{-1}, \quad (2.6)$$

where \tilde{H}_M is the $(2nM) \times (2nM)$ coupling matrix between the surface orbitals of the leads, which can be obtained by recursive decimation of the Hamiltonian $H_{LM} + H_M + H_{MR}$. Finally for a given G^S the scattering matrix elements can be obtained using a variant of the Fisher-Lee relations [22]. In order to highlight the efficiency of this approach in the case of disorder multilayers, we briefly describe how the decimation technique recursively eliminates all the internal degrees of freedom of the multilayer to yield the reduced matrix \tilde{H}_M coupling surface states of the leads. Suppose the total number of degrees of freedom of the Hamiltonian $H_{LM} + H_M + H_{MR}$ is N . It is possible to eliminate the $i = 1$ degree of freedom by reducing the $N \times N$ total Hamiltonian to an $(N - 1) \times (N - 1)$ matrix with elements

$$H_{ij}^{(1)} = H_{ij} + \frac{H_{i1}H_{1j}}{E - H_{11}}. \quad (2.7)$$

Repeating this procedure l times, we obtain the decimated Hamiltonian at l -th order

$$H_{ij}^{(l)} = H_{ij}^{(l-1)} + \frac{H_{il}^{(l-1)} H_{lj}^{(l-1)}}{E - H_{ll}^{(l-1)}} , \quad (2.8)$$

and after $N - nM$ iterations we obtain the $(nM) \times (nM)$ effective Hamiltonian

$$\tilde{H}_M(E) = \begin{pmatrix} \tilde{H}_L^*(E) & \tilde{H}_{LR}^*(E) \\ \tilde{H}_{RL}^*(E) & \tilde{H}_R^*(E) \end{pmatrix} . \quad (2.9)$$

In this expression the matrices $\tilde{H}_L^*(E)$ and $\tilde{H}_R^*(E)$ describe the intra-surface couplings respectively in the left and right surfaces, and $\tilde{H}_{LR}^*(E)$ and $\tilde{H}_{RL}^*(E)$ describe the effective coupling between these surfaces. From equations (2.7) and (2.8) it is clear that only matrix elements coupled to the eliminated degree of freedom are redefined. Hence the recursive technique becomes very efficient in the case of short-range interactions, particularly in the case of nearest neighbor tight-binding models. Consider now a disordered multilayer composed of alternating magnetic (M) and non-magnetic (N) layers of thicknesses t_M and t_N respectively. Suppose that the multilayer consists of μ repeated (N/M/N/M) units, that we call double bilayers (DB). Since we consider only short range interactions, it is possible to decimate the Hamiltonian of the whole multilayer by building up the following intermediate Hamiltonian

$$H_M = \begin{pmatrix} \dots & \dots & \dots & \dots & \dots & \dots & \dots & \dots \\ V_0^\dagger & H_{Li} & H_{LRi} & 0 & \dots & \dots & \dots & \dots \\ \dots & H_{RLi} & H_{Ri} & V_0 & 0 & \dots & \dots & \dots \\ \dots & 0 & V_0^\dagger & H_{L(i+1)} & H_{LR(i+1)} & 0 & \dots & \dots \\ \dots & 0 & 0 & H_{RL(i+1)} & H_{R(i+1)} & V_0 & 0 & \dots \\ \dots & \dots & \dots & \dots & \dots & \dots & \dots & \dots \\ \dots & \dots & \dots & \dots & \dots & \dots & \dots & \dots \end{pmatrix} , \quad (2.10)$$

where H_{Li} (H_{Ri}) describe the coupling within the left (right) hand surfaces of the i -th cell (N/M/N/M) ($i=1, \dots, \mu$), H_{LRi} ($H_{RLi} = H_{LRi}^\dagger$) describe the coupling between the left and right surfaces of the i -th cell, and V_0 is the “bare” coupling between the first right-hand atomic plane of the i -th cell and the first left-hand atomic plane of the $(i+1)$ -th cell, which is assumed to be the same for every cell (this last condition is easily satisfied if the first left-hand and the last right-hand atomic plane of every (N/M/N/M) cell is disorder-free). Equation (2.10) suggests a very convenient implementation in which multilayers consisting of μ (N/M/N/M) cells are built using the following procedure. Firstly we decimate a certain number ν , of cells (N/M/N/M) in which disorder is introduced everywhere except in the first and last atomic plane. Secondly the matrix H_M of equation (2.10) is built, choosing randomly the order of the μ (N/M/N/M) cells. Finally the matrix H_M is further decimated to yield \tilde{H}_M . Note that μ^ν possible different multilayers can be built from a set of ν disordered unit cells, and that the computation time scales as the number of (N/M/N/M) cells and not as the total length of the scatterer. This procedure can be further optimized, for instance by building ν' new cells (N/M/N/M) $\times 2$, and using these to form the multilayers. This turns out to be useful in the case of very long samples.

The technique for computing transport properties, is based on a three dimensional tight-binding model with nearest neighbor couplings on a simple cubic lattice and two degrees of freedom per atomic site. The general spin-dependent Hamiltonian is

$$H^\sigma = \sum_{i,\alpha} \epsilon_i^{\alpha\sigma} c_{\alpha i}^{\sigma\dagger} c_{\alpha i}^\sigma + \sum_{i,j,\alpha\beta} \gamma_{ij}^{\alpha\beta\sigma} c_{\beta j}^{\sigma\dagger} c_{\alpha i}^\sigma , \quad (2.11)$$

where α and β label the two orbitals (which for convenience we call s and d), i, j denote the atomic sites and σ the spin. $\epsilon_i^{\alpha\sigma}$ is the on-site energy which can be written as $\epsilon_i^\alpha = \epsilon_0^\alpha + \sigma h \delta_{\alpha d}$ with h the exchange energy and $\sigma = -1$ ($\sigma = +1$) for majority (minority) spins. In equation (2.11), $\gamma_{ij}^{\alpha\beta\sigma} = \gamma_{ij}^{\alpha\beta}$ is the hopping between the orbitals α and β at sites i and j , and $c_{\alpha i}^\sigma$ ($c_{\alpha i}^{\sigma\dagger}$) is the annihilation (creation) operator for an electron at the atomic site i in an orbital α with a spin σ . h vanishes in the non-magnetic metal, and $\gamma_{ij}^{\alpha\beta}$ is zero if i and j do not correspond to nearest neighbor sites. Hybridization between the s and d orbitals is taken into account by the non-vanishing term γ^{sd} . We have chosen to consider two orbitals per site in order to give an appropriate description of the density of states of transition metals and to take into account inter-band scattering occurring at interfaces between different materials. The DOS of a transition metal consists of narrow bands (mainly d -like) embedded in broader bands (mainly sp -like). This feature can be reproduced in the two-band model, as shown in figure 1. The position of the Fermi energy with respect to the edge of the d band determines the transport properties of pure transition metals. For instance the current in silver is carried almost entirely by light effective mass sp electrons with a small DOS, while in the minority band of Co or

Ni it is carried by heavy d electrons with a large DOS. The hybridization at the Fermi energy can also be important and for instance in copper the current consists of an equal mixture of sp and d electrons. In our earlier analysis of the material dependence of CPP GMR [19] we identified large inter-band scattering as one of the main sources of GMR. In particular we have shown that due to inter-band scattering the conductance of a multilayer in the anti-parallel configuration is always smaller than both spin conductances in the parallel configuration. It is possible to capture this feature by choosing the parameters of the two-band model to yield conductances as close as possible to those obtained for the full spd model [19]. In the case of a heterojunction, the hopping parameters between different materials are chosen to be the geometric mean of the hopping elements of the bulk materials. The parameters for Cu and Co are presented in Table I. In figure 2 we show the corresponding normalized conductance for Co/Cu multilayers attached to semi-infinite Cu leads as a function of the Cu layer thickness. We notice that as a consequence of inter-band scattering the conductance in the anti-parallel configuration is always the smallest, a feature which is not present in a simple single-band model. We believe this simple two-band model is the minimal model capable of describing in a semi-quantitative way the behavior of transition metals because it includes the correct DOS and the possibility of scattering electrons between high dispersion (s) and low dispersion bands (d).

B. Models of Disorder

Figure 3 shows the different models of disorder analyzed below. The simplest model was introduced by Anderson within the framework of the localization theory [23] and consists of adding a random potential V to each on-site energy, with a uniform distribution of width W ($-W/2 \leq V \leq W/2$), centered on $V = 0$

$$\tilde{\epsilon}_i^{\alpha\sigma} = \epsilon_i^{\alpha\sigma} + V. \quad (2.12)$$

This generic model of disorder can yield arbitrary mean free paths and significant spin-asymmetry in the conductance. To obtain a more realistic description of disorder we also consider the rôle of lattice distortions, which are known to be present at the interfaces between materials with different lattice constants. Moreover in the case of electrodeposited nanowires, contamination by impurities is unavoidable, and lattice distortions occur in the vicinity of such point defects. In what follows we model lattice distortions by scaling the hopping parameters between nearest neighbors. It has been proposed [24] and confirmed numerically [25] that the following scaling law for the tight-binding hopping $\gamma^{\alpha\beta}$ is valid

$$\gamma^{\alpha\beta} = \gamma_0^{\alpha\beta} \cdot (1 + \delta r)^{-(1+\alpha+\beta)}, \quad (2.13)$$

where $\gamma_0^{\alpha\beta}$ is the hopping element for atoms at the equilibrium positions r_0 , α and β are the angular momenta of the orbitals forming the bond, and δr is the displacement from the equilibrium position relative to r_0 ($\delta r = \Delta r/r_0$ with Δr the displacement from the equilibrium position). Hence the s - s hopping scales as $(1 + \delta r)^{-1}$, the d - d as $(1 + \delta r)^{-5}$ and the s - d as $(1 + \delta r)^{-3}$. Note that it has been recently proved [26] that in 3d transition metals contaminated with 3d and 4sp impurities the variation of the nearest neighbor distance in the proximity of an impurity never exceeds $\sim 5\%$, which is within the limit of validity of equation (2.13). In the following we will consider uniform distributions of lattice displacements with zero mean.

As mentioned above, in electrodeposited GMR nanowires, because of the dual-bath deposition technique, the magnetic layers are contaminated by non-magnetic impurities up to 15% in concentration [27], while a negligible concentration of magnetic impurity atoms is present in the non-magnetic layers. To describe this feature we have introduced non-magnetic impurities in the magnetic layers of the multilayer. An impurity is modeled by substituting a magnetic ion by a non-magnetic ion (ie Cu instead of Co for the materials considered) at an atomic site. The on-site energy of the impurity is assumed to be the same as the bulk material forming the impurity (ie bulk Cu for Cu impurities), and the hopping tight-binding parameters depend on the type of sites surrounding the impurity. We do not introduce correlation between impurities and hence there are no clustering effects. Although this model is quite primitive and does not take into account perturbations of atoms in the proximity of the impurity, density functional calculations [28] have shown that a good estimate of the resistivity of transition metal alloys in the low concentration limit is possible by considering only perturbations of the first nearest neighbors of the impurity. This suggests that our simple models should give a correct qualitative description of a 3d impurity in 3d transition metals.

As a third source of disorder we have considered the possibility of vacancies. A vacancy is introduced simply by setting an on-site energy to a large number, with all the hoppings to nearest neighbors set to zero. We do not consider aggregation of vacancies and assume a uniform distribution across the whole multilayer. Finally we model cross-section fluctuations of GMR nanowires by examining a wire of finite cross-section which is not repeated periodically in the transverse direction and mimic the fluctuations along the wire by introducing vacancies in the first monolayer at the wire surface.

In all the calculations with disorder, we consider finite cross-sections involving 5×5 atomic sites, which we repeat periodically using up to 100 k_{\parallel} -points in the 2D Brillouin zone. In the case of cross-section fluctuations we compute the ensemble-averaged conductance of wires with finite cross-sections as large as 15×15 atomic sites. It is important to note that in sputtered or MBE multilayers the typical cross-sections vary between $1\mu\text{m}^2$ and 1mm^2 , which is several times larger than the typical phase breaking length l_{ph} . On the other hand in the case of electrodeposited nanowires the diameter of the wires is usually between 20nm and 90nm, but several wires are measured at the same times thereby yielding the mean conductance of an array of phase coherent nanowires, each with a cross-section of the order of l_{ph}^2 .

III. RESULTS AND DISCUSSION

A. Disorder-induced enhancement of the spin-conductance asymmetry

In this section we consider effects produced by Anderson-type disorder, impurities and lattice distortions. Despite the fact that the disorder in each of these cases is spin-independent the effect on transport is spin-dependent. In order to investigate the different conductance regimes that may occur and their dependence on the magnetic state of the system it is convenient to consider as a scaling quantity the average spin conductance $\langle \Gamma^{\sigma} \rangle$ multiplied by the total multilayer length L and divided by the number of open scattering channels in the leads. We define the resulting “reduced” conductance g by means of the equation

$$g^{\sigma} = \frac{h}{e^2} \frac{\langle \Gamma^{\sigma} \rangle}{N_{\text{open}}} \cdot L, \quad (3.1)$$

where the number of open channels in the leads N_{open} in the case of a finite system is proportional to the multilayer cross-section. In the ballistic limit g increases linearly with a coefficient proportional to the conductance per unit area, in the diffusive (metallic) limit g is constant, and in the localized regime g decays as $g \propto \exp(-L/\xi)$ with ξ the localization length [29,30]. Consider first the case of a random on-site potential. For Co/Cu multilayers with a width of disorder $W = 0.6\text{eV}$, figure 4 shows the quantity g in units of e^2/h for the two spin sub-bands in the P and AP configurations along with the ratio $\eta = g_{\text{P}}^{\uparrow}/g_{\text{P}}^{\downarrow}$. These results were obtained for a cross-section of 5×5 atoms, and layer thicknesses of $t_{\text{Cu}} = 8$ atomic planes (AP) and $t_{\text{Co}} = 15\text{AP}$. In figure 4 the standard deviation of the mean is negligible on the scale of the symbols, and each point corresponds to an additional Cu/Co double bilayer. From the figure it is immediately clear that the spin-asymmetry of g (ie of the conductance) is increased by the disorder, which as a consequence of the band structure, turns out to be more effective in the minority band and in the AP configuration. In fact the disorder has the effect of spreading the DOS beyond the band edge, but does affect the centre of the band. The relevant quantity is the disorder strength defined as the ratio r_{α} between the width of the distribution of random potentials and the band width $r_{\alpha} = W/\gamma_{\alpha}$. For the set of parameters that we have chosen the disorder strength of the s and d band is respectively $r_d = 0.7$ and $r_s = 0.22$. Since the current in the majority band of the P configuration is carried mostly by s electrons, for which the disorder strength is weak, the majority spin sub-band will not be strongly affected by the disorder. In contrast in the minority band and in both bands in the AP configuration, the current is carried by d electrons, for which the scattering due to disorder is strong.

A second remarkable result is that in the P configuration the almost ballistic majority electrons can co-exist with diffusive minority carriers. In the regime of phase coherent transport the definition of spin-dependent mean free paths for individual materials within the multilayer is not meaningful, and one must consider the spin-dependent mean free path for the whole multilayered structure. Hence we introduce the elastic mean free path for the majority (minority) spin sub-band in the P configuration $\lambda_{\text{P}}^{\uparrow}$ ($\lambda_{\text{P}}^{\downarrow}$) and for both spins in the AP configuration $\lambda_{\text{AP}}^{\uparrow\downarrow}$. This is defined as the length at which the corresponding conductance curve $g(L)$ changes from linear to constant (ie the length L^* corresponding to the crossing point between the curve $g(L)$ and the tangent to g in the region where g is constant). For the calculation in figure 4 we estimate $\lambda_{\text{P}}^{\uparrow} > 3000\text{AP}$, $\lambda_{\text{P}}^{\downarrow} \sim 500\text{AP}$ and $\lambda_{\text{AP}}^{\uparrow\downarrow} \sim 1000\text{AP}$. All of these results are obtained at zero temperature and voltage. At finite temperature, when the phase breaking length l_{ph} is shorter than the elastic mean free path, l_{ph} becomes the length scale of the system. It is possible to generalize the Landauer-Büttiker approach to the transport in presence of finite phase breaking length [31]. In this case the system can be considered as a series of phase coherent scatterers of length l_{ph} , added in series through reservoirs that make the phases random, and the scattering properties of such a structure are solely determined by elastic transport up to a length l_{ph} . If the loss of coherence occurs on length scales longer than the individual layer thicknesses t_{Co} and t_{Cu} , the standard resistor approach is not valid, and aggregate of cells as long as l_{ph} are the appropriate quantities to add in series.

Turning now our attention to GMR, it is clear from figure 4 and equation (2.2) that enhanced spin asymmetry will increase the GMR ratio because of the high transmission in the majority band. In figure 5 we present the GMR

ratio as a function of the total multilayer length for different values of the width of the distribution of the random potential. From the figure we conclude that GMR strongly increases as a function of the disorder strength and that this is due to the increasing of the spin polarization of the conductance. We also notice that the standard deviation of the mean GMR increases as a function of disorder and of the multilayer length. This is due to the approaching of the AP conductance to the localized regime, in which the fluctuations are expected to be large. The results of figures 5 seem to be in contradiction with the published results of Tsymbal and Pettifor [17]. In that case an analogous kind of disorder was employed together with an accurate *spd* tight-binding model, and the GMR ratio turned out to decrease with increasing disorder. They calculated the conductance for an infinite diffusive system using a small disordered unit cell in the direction of the current, namely a Co_4/Cu_4 cell (the subscripts indicate the number of atomic planes). To check this apparent contradiction we have calculated the conductances and the GMR ratio for a $\text{Co}_5/\text{Cu}_5/\text{Co}_5/\text{Cu}_5$ unit cell attached to pure crystalline Cu leads. Apart from the resistances of the interfaces with the leads, the conductance for this system is proportional to the conductance calculated in ref [17] and figure 6 shows that the GMR ratio for such a short system does indeed decrease with disorder strength. This shows that for small cells, when the mean free path is much longer than the cell itself, the increase of all the resistances is not fully compensated by an increase of their spin-asymmetry, and this gives rise to a decrease of GMR. In contrast for thicker layers, provided the transport remains phase coherent, asymmetry builds up with increasing L and the resulting GMR ratio increases.

Consider now the effect produced by Cu impurities in the Co layers and by lattice distortions. The main features of both these kinds of disorder are very similar to the case of a random on-site potential: the GMR ratio increases as a function of disorder because of an increase in spin-asymmetry. Again the quantity g behaves quasi-ballistically for small lengths, followed by a diffusive region and finally by a localized regime. The mean free path at any disorder turns out to be longer for the majority spins in the P configuration and the co-existence of ballistic majority electrons with diffusive minority electrons is still possible. This means that even in these cases spin-independent disorder produces spin-dependent effects. Similar arguments to the one used for the on-site random potential can be applied. In fact, in the case of impurities, we note from Table I that the alignment between the majority band of Co and the conduction band of Cu is better than that of the minority band of Co. Hence impurities are less effective in the majority band than in the minority. For lattice distortions, it is important to observe that the scaling of the hopping coefficients with the displacement from the equilibrium position is more severe for the d orbitals (see equation (2.13)). Since the current in the majority band is s -like while in the minority band and in the AP configuration it is d -like, this different scaling will result in larger disorder-induced scattering for the minority channel and for the AP configuration. Figure 7 shows the reduced conductances g for all the the spins in the case of uniform distributions of lattice displacements with different widths. From the figure we can conclude that: i) the spin-conductance asymmetry increases with increasing disorder ii) all the mean free paths decrease, iii) the contrast between $g_{\text{P}}^{\downarrow}$ and $g_{\text{P}}^{\uparrow\downarrow}$ increases with disorder.

We wish to conclude this paragraph with some final remarks about length scales involved. As mentioned above, since we are dealing with phase coherent transport, the concept of mean free path within the individual layers loses meaning, and we can only speak about the spin-dependent mean free path of the whole multilayer (ie $\lambda_{\text{P}}^{\uparrow}$, $\lambda_{\text{P}}^{\downarrow}$ and $\lambda_{\text{AP}}^{\uparrow\downarrow}$). Nevertheless, if the mean free paths of both the spin sub-bands in the P configuration extend over a length scale comparable with the cell Co/Cu ($\lambda_{\text{P}}^{\uparrow}, \lambda_{\text{P}}^{\downarrow} \sim t_{\text{Co}} + t_{\text{Cu}}$), the mean free path of the AP configuration is simply given by

$$\lambda_{\text{AP}}^{\uparrow\downarrow} = \frac{\lambda_{\text{P}}^{\uparrow} + \lambda_{\text{P}}^{\downarrow}}{2}, \quad (3.2)$$

and a resistor network approach becomes valid. We have checked this prediction by calculating the GMR ratio as a function of the number of double bilayers for multilayers with different Co layer thicknesses but the same concentration of impurities (8%). By increasing the Co thickness we can cross over from a regime in which the resistor network is not valid at the scale of the bilayer thickness to a regime in which the resistances of bilayers add in series. In the first case we expect that the GMR ratio will increase as the number of bilayers increases and in the second we expect a constant GMR. The result for a Co thicknesses of respectively 150AP, 50AP and 15AP is presented in figure 8. Note that for a phase-coherent structure the increase of GMR with the number of bilayers is different from the increase of GMR in diffusive systems when the total multilayer length is kept constant (as predicted by the Boltzmann approach [10] and observed experimentally [6,7,12]). In the latter case the effect is due to an interplay between the resistances of the different materials while in the former it is due to an increase of the spin asymmetry of the current. To date an increase of GMR with the number of bilayers has been observed in the CIP configuration [32], while the same measurements in the CPP configuration are still in progress [33].

B. Reduction of mean free path

In this section we consider the effect of vacancies and cross-section fluctuations and their interplay with other sources of disorder discussed in the previous section. We recall that cross-section fluctuations are modeled as vacancies with a distribution concentrated at the boundaries of a finite cross-section multilayer. Hence we expect the qualitative behavior of vacancies and cross-section fluctuations to be the same. These sources of disorder do not act on the two spin sub-bands in a selective way and produce only a small spin asymmetry. The main effect is to drastically reduce the elastic mean free paths of all the spins. In figure 9 we present the reduced spin conductances g^σ , the spin asymmetry η and the GMR ratio for a Co/Cu multilayer ($t_{\text{Cu}} = 8\text{AP}$, $t_{\text{Co}} = 15\text{AP}$) with a vacancy concentration of 1%. The results obtained for cross-section fluctuations are very similar and are not shown here. Figure 9 shows that (in contrast with figure 4b) the spin asymmetry of the conductance is not greatly enhanced by the presence of vacancies. For the parameters used in the present simulation η varies from 1.6 to 3.5 for multilayers with a total thickness ranging from 46 to 3000 atomic planes. In contrast for the case of a random on-site potential of 0.6eV figure 4 shows that η varies from 2 to about 30 for the same range of multilayer lengths. Moreover we notice that in the case of a random on-site potential the spin asymmetry of the current is always larger than in the disorder-free case. In contrast, when vacancies are present, the spin asymmetry of the current is smaller than the disorder-free case for short multilayers and becomes larger for longer multilayers. From figure 9 we can see that the cross-over length (that we denote l_{cr}), defined as the length at which η for a system with vacancies equalizes η for the disorder-free case, is comparable with the mean free path of the minority spins in the P configuration and of the AP configuration. It is important to note that the reduction of all the mean free paths with respect to the vacancy concentration is very severe. The reduced spin conductances g exhibit quasi-ballistic behavior for lengths up to l_{cr} , and an almost localized behavior for lengths larger than l_{cr} . The diffusive region is strongly suppressed and there is a small difference between all the spin-dependent elastic mean free paths. The spin asymmetry of the current can be enhanced by increasing the vacancy concentration, but this produces a further decreasing of the mean free paths and a further suppression of the diffusive region, resulting in a global reduction of GMR for lengths shorter than l_{cr} . For lengths longer than l_{cr} GMR is enhanced and this is due to the approach of $g_{\text{AP}}^{\uparrow\downarrow}$ to the localized regime. To date there is no evidence of localization effects in metallic magnetic multilayers and we believe that our results are currently important only for lengths shorter than l_{cr} . To summarize, the main effects of vacancies are, on the one hand to reduce the spin asymmetry of the current for lengths shorter than l_{cr} and to enhance it for lengths larger than l_{cr} , and on the other to reduce drastically the mean free paths for all the spins in both magnetic configurations. The cross-over length is comparable with the mean free path of the minority spin in the P configuration and GMR is always reduced in the limit of quasi-ballistic transport.

The qualitative results obtained for vacancies are broadly mirrored by those of cross-section fluctuations, although there are some differences. The simulations with cross-section fluctuations have been carried out with a finite cross-section, whereas for the case of vacancies where we have considered a wire repeated periodically in the transverse direction. When cross-section fluctuations are introduced, the disorder-induced scattering scales as $P/S \propto 1/L$ with P the perimeter, S the area of the cross-section and $L = \sqrt{S}$. This introduces a new length scale, namely the cross-section linear dimension $l_{\text{cs}} = \sqrt{S}$. If this length is shorter than the mean free paths, then a reduction of GMR will take place for the same reasons as in the case of vacancies, whereas if the mean free paths are shorter than l_{cs} , the effect of the cross-section fluctuations will be weak and no further reduction of the GMR will take place. Unfortunately, even with the optimized technique presented in the previous section it is very difficult to investigate the limit $\lambda \leq l_{\text{cs}}$. We have performed simulations with cross-sections up to 15×15 atomic sites, which is far below this limit, and have found no important deviations from the case of vacancies. A cross-section of 15×15 atomic sites corresponds to P/S of $0.26a_o^{-1}$ with a_o the lattice constant. This is comparable with the values of experiments [5–7] which we estimate range between $0.005a_o^{-1}$ and $0.025a_o^{-1}$. This suggests that the disorder strength in our simulations is larger than experimental values and that the effects of the cross-section fluctuations on GMR nanowires should be weak. On the other hand our model for cross-section fluctuations involves only the first monolayer at the boundaries while in real systems the roughness extends over several monolayers. Moreover long range correlated surface roughness along the wires is likely to be present in real systems because of the structure of the nano-holes in which the wires are deposited. All these effects may result in a drastic enhancement of the disorder strength due to surface roughness and therefore a reduction of GMR.

A key result of the above simulation is that the reduction of GMR due to vacancies and cross-section-fluctuations may be compensated by a large increase of the spin asymmetry of the conductance. To address this issue we have performed simulations with both vacancies and non-magnetic impurities in the magnetic layers. The GMR ratios and spin asymmetries of the conductances are presented in figure 10 for Co/Cu multilayers with different impurities and vacancies concentrations. The figures shows very clearly that competing effects due to impurities and vacancies can give rise to large values of GMR even for very disordered systems. The same value of GMR obtained in presence

of impurities and vacancies can be obtained for a system with only impurities, but at a lower concentration. The fundamental difference between the two cases is that when impurities and vacancies co-exist, all the mean free paths are very small and the large GMR is solely due to the large spin asymmetry of the current.

IV. CONCLUSIONS

Due to the development of improved deposition techniques, recent experiments [33,34] have revealed the need for a description of phase coherent transport, which goes beyond the diffusive approach. We have addressed this issue by extending a previously developed technique [19] to the case of disordered systems, where large ensemble averages are needed. We have presented several models of disorder within a two-band tight-binding model on a simple-cubic lattice. The model, despite its simplicity, can capture the relevant aspects of transition metal multilayers and can provide a general understanding of spin-dependent phase-coherent transport. Moreover, because of the high efficiency of the technique, we have been able to investigate very long systems, different transport regimes (ballistic, diffusive and localized) and the cross-over between them.

We have shown that impurities, random on-site potentials and lattice distortions reduce the spin-dependent mean free paths, but at the same time increase the spin-asymmetry of the current and the GMR ratio. In contrast, vacancies and cross-section fluctuations drastically reduce all the spin-dependent mean free paths without largely increasing the spin asymmetry of the current, and this produces a decrease of the GMR, at least far away from the strong localized regime. Nevertheless the effect of vacancies can be compensated by increasing the spin asymmetry (for instance with impurities) and this can account for the large GMR of electrodeposited nanowires.

Acknowledgments: This work is supported by the EPSRC, the EU TMR Programme and the DERA.

-
- [1] M.N.Baibich, J.M.Broto, A.Fert, F.Nguyen Van Dau, F.Petroff, P.Etienne, G.Creuzet, A.Friederich, and J.Chazelas, Phys. Rev. Lett. **61**, 2472 (1988);
 - [2] G.Binasch, P.Grünberg, F.Sauerbach and W.Zinn, Phys. Rev. **B 39**, 4828 (1989)
 - [3] W.P.Pratt Jr., S.-F.Lee, J.M.Slaughter, R.Loloe, P.A.Schroeder, J.Bass, Phys. Rev. Lett. **66**, 3060 (1991)
 - [4] M.A.M.Gijs, S.K.J.Lenczowski, J.B.Giesbers, Phys. Rev. Lett. **70**, 3343 (1993)
 - [5] W.Schwarzacher, D.S.Lashmore, IEEE Trans. Magn. **32**, 3133 (1996)
 - [6] A.Blondel, J.P.Meier, B.Doudin, J.Ph.Ansermet, Appl. Phys. Lett. **65**, 3019 (1994)
 - [7] L.Piroux, S.Dubois, A.Fert, L.Belliard, Eur. Phys. J. **B 4**, 413 (1998)
 - [8] M.A.M.Gijs, G.E.W.Bauer, Adv. Phys., **46**, 285 (1997)
 - [9] J-Ph. Ansermet, J.Phys.: Cond. Matter **C 10**, 6027 (1998)
 - [10] T.Valet, A. Fert, Phys. Rev. **B 48**, 7099 (1993)
 - [11] A. Fert, J.-L. Duvail, T.Valet, Phys.Rev. **B 52**, 6513 (1995)
 - [12] S.-F.Lee, W.P.Pratt Jr., R.Loloe, P.A.Schroeder, J.Bass, Phys. Rev. **B 46**, 548 (1992)
 - [13] P.Zahn, J.Binder, I.Mertig, R.Zeller, P.H.Dederichs, Phys. Rev. Lett. **80**, 4309 (1998)
 - [14] P.Zahn, I.Mertig, M.Richter, H.Eschrig, Phys. Rev. Lett. **75**, 2996 (1995)
 - [15] K.M.Schep, P.J.Kelly, and G.E.W.Bauer, Phys. Rev. Lett. **74**, 586 (1995)
 - [16] K.M.Schep, P.J.Kelly, and G.E.W.Bauer, Phys. Rev. **B 57**, 8907 (1998)
 - [17] E.Yu.Tsymbal and D.G.Pettifor, Phys. Rev. **B 54**, 15314 (1996).
 - [18] J.Mathon, Phys. Rev. **B 55**, 960 (1997)
 - [19] S.Sanvito, C.J.Lambert, J.H.Jefferson, and A.M.Bratkovsky, accepted for publication in Phys.Rev. **B**, also cond-mat/9808282
 - [20] S.Sanvito, C.J.Lambert, J.H.Jefferson, and A.M.Bratkovsky, J. Phys.C: Condens. Matter, **10**, L691 (1998)
 - [21] M.Büttiker, Y.Imry, R.Landauer, and S.Pinhas, Phys. Rev. **B 31**, 6207 (1985)
 - [22] C.J.Lambert, V.C.Hui, S.J.Robinson, J.Phys.C: Condens. Matter, **5**, 4187 (1993)
 - [23] P.W.Anderson, D.J.Thouless, E. Abrahams, D.S.Fisher, Phys.Rev. **B 22**, 3519 (1980)
 - [24] O.K.Andersen, O.Jepsen, Physica **B 91**, 317 (1977)
 - [25] D.A.Papaconstantopoulos, *Handbook of the Band Structure of Elemental Solids*, (Plenum, New York, 1986)
 - [26] N.Papanikolaou, R.Zeller, P.H.Dederichs, N.Stefanou, Phys. Rev. **B 55**, 4157 (1997)
 - [27] B.Voegeli, A.Blondel, B.Doudin, J.Ph.Ansermet, J. Magn. Magn. Mater, **151**, 388 (1995)

- [28] I.Mertig, R.Zeller, P.H.Dederichs, Phys. Rev. **B 47**, 16178 (1993)
- [29] C.W.J. Beenakker, Rev. Mod. Phys. **69**, 731 (1997)
- [30] B. Kramer, A. MacKinnon, Rep. Prog. Phys. **56**, 1469 (1993)
- [31] M. Büttiker, Phys. Rev. **B 3**, 3020 (1986)
- [32] C. Marrows, PhD dissertation, University of Leeds, (1997)
- [33] D. Bozec, C. Marrows, B. Hickey, M. Howson, private communication
- [34] W.-C. Chiang, Q. Yang, W. P. Pratt Jr., R. Loloee, J. Bass, J. Appl. Phys. **81**, 4570 (1997)

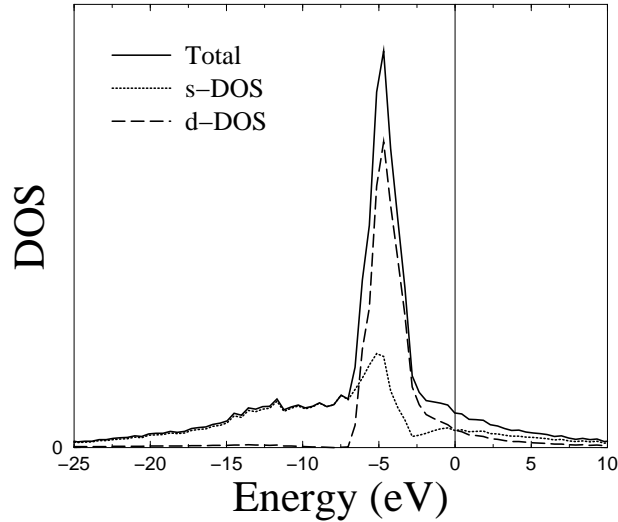


FIG. 1. DOS obtained for the two-band model. The parameters used are the ones corresponding to Cu in the Table I. The vertical line denotes the position of the Fermi energy used in the calculation

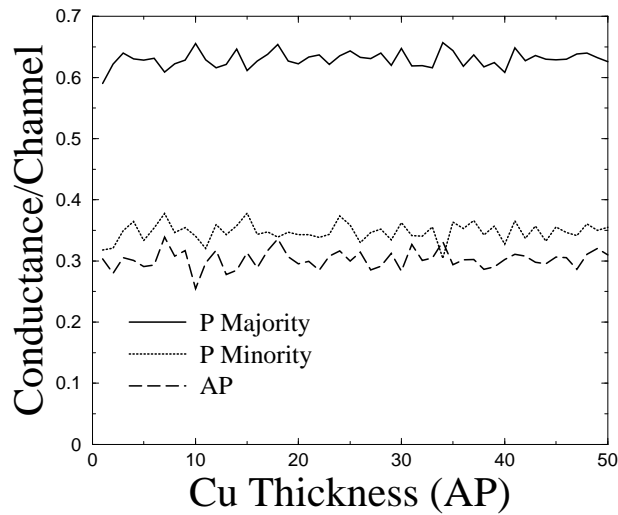


FIG. 2. Conductances normalized to the number of open channels for Co/Cu multilayers with Cu semi-infinite leads as a function of the Cu layers thickness. This gives rise to a GMR of about 60%.

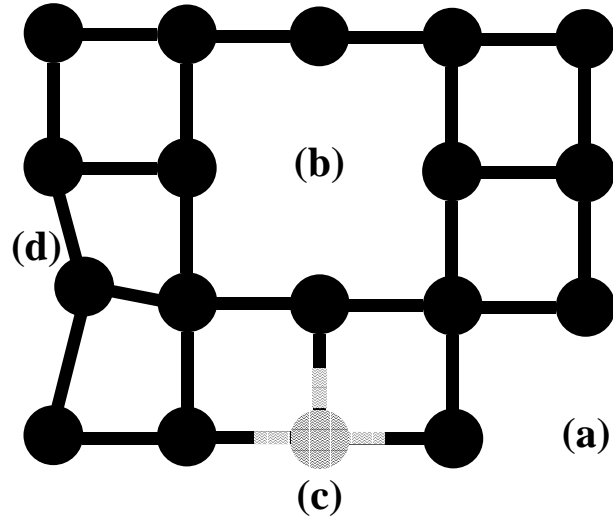


FIG. 3. Schematic illustration of the disorder models considered: (a) vacancy at the boundary of the cell (cross-section fluctuation), (b) vacancy in the bulk, (c) impurity (with hopping parameters the geometric mean of those for bulk and the impurity), (d) lattice distortion.

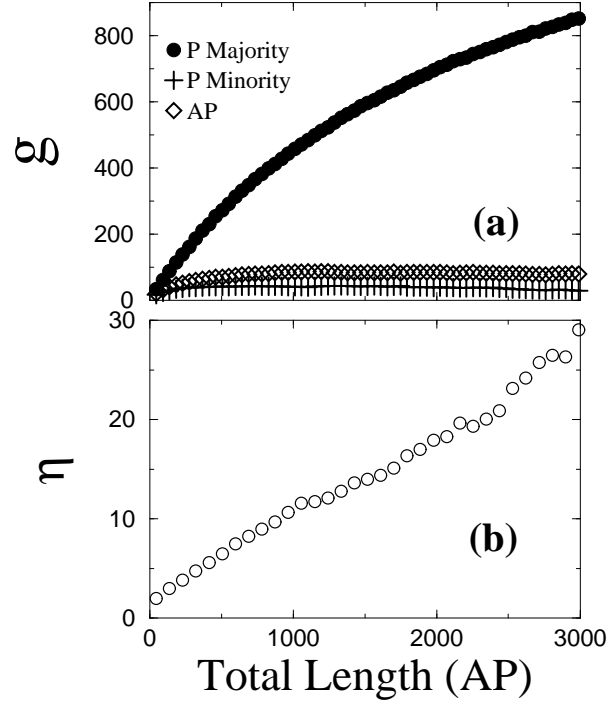


FIG. 4. Reduced conductance g^σ and spin asymmetry $\eta = g_P^\uparrow / g_P^\downarrow$ as a function of the multilayer length for Cu/Co multilayers with random on-site potential. The random potential has a normal distribution of width 0.6eV, and the layer thicknesses are $t_{\text{Cu}} = 8\text{AP}$ and $t_{\text{Co}} = 15\text{AP}$. Each point corresponds to a cell Co/Cu/Co/Cu of total thickness 46AP.

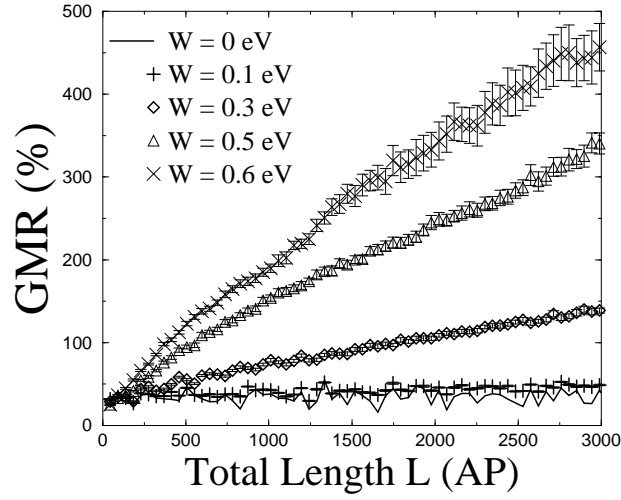


FIG. 5. GMR as a function of the total multilayer length for different values of the on-site random potential. The layer thicknesses are $t_{\text{Cu}} = 8\text{AP}$ and $t_{\text{Co}} = 15\text{AP}$ and each point corresponds to a cell Co/Cu/Co/Cu of total thickness 46AP.

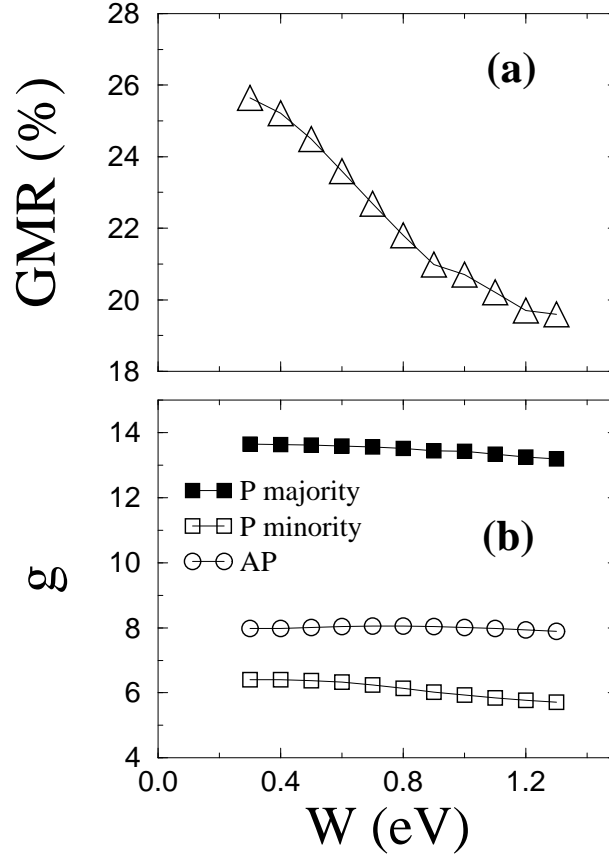


FIG. 6. GMR and reduced spin conductances as a function of the width W of the normal distribution of on-site random potentials for a single Co/Cu/Co/Cu cell with Co and Cu thicknesses of 5AP.

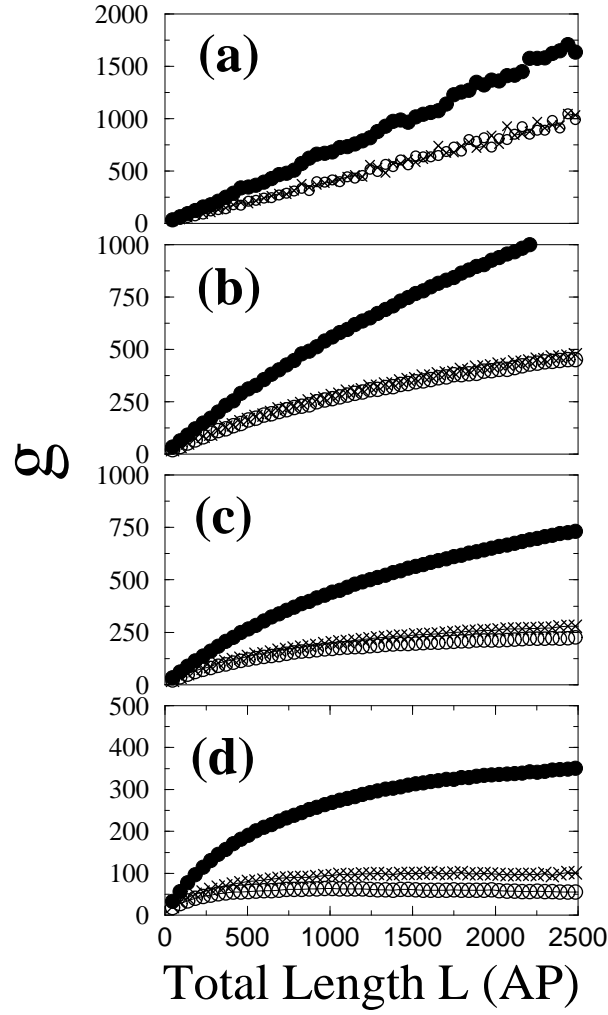


FIG. 7. Reduced spin conductances g for different width of a normal distribution of lattice distortion: (a) $\delta r = 0$, (b) $\delta r = 0.02\%$, (c) $\delta r = 0.03\%$, (d) $\delta r = 0.05\%$. The symbols \bullet (\circ) represent the majority (minority) spins in the P configuration, and \times the AP configuration. The layer thicknesses are $t_{\text{Cu}} = 8\text{AP}$ and $t_{\text{Co}} = 15\text{AP}$ and each point corresponds to a cell Co/Cu/Co/Cu of total thickness 46AP. Note the different vertical scales for the different disorders.

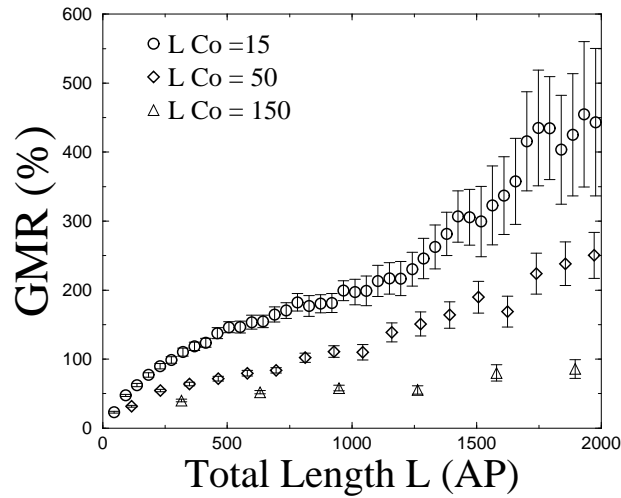


FIG. 8. GMR as a function of the number of double bilayers for an impurity concentration of 8%. The Cu thickness is fixed to 8AP and the Co thickness is varied in order to show the cross-over from a phase coherent regime to a regime in which a resistor network model is valid. Note that in the case of $t_{\text{Co}} = 150\text{AP}$ the GMR is almost independent of the total multilayer length.

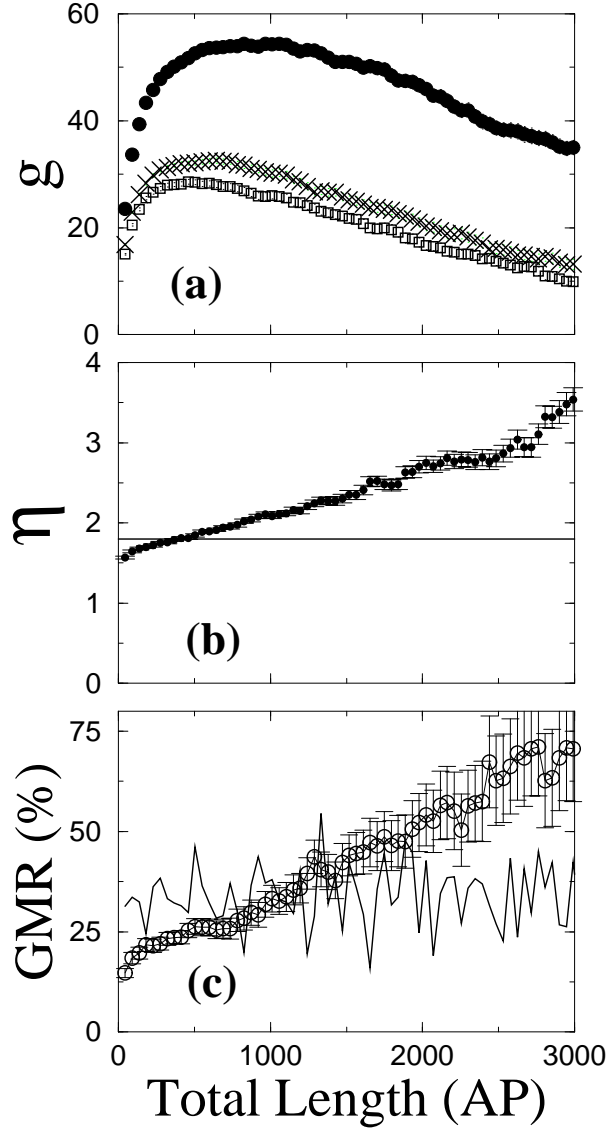


FIG. 9. Effects of vacancies on Co/Cu multilayers. Figure (a) shows the reduced spin conductance for majority spin in the P configuration (●), for minority spins in the P configuration (□), and for the AP configuration (×). Figure (b) shows the spin asymmetry of the conductance and figure (c) the GMR. The horizontal line of (b) represents the average spin asymmetry of the conductance for the clean system. In figure (c) the symbols ○ represent the system with vacancies and the solid line the disorder-free system. The vacancy concentration is 1% and the thicknesses are $t_{\text{Cu}} = 8\text{AP}$ and $t_{\text{Co}} = 15\text{AP}$.

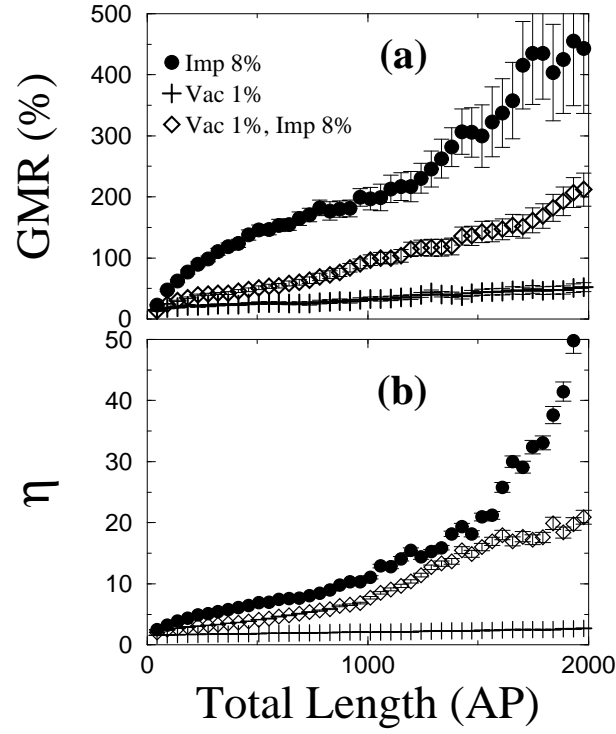


FIG. 10. Competition between vacancies and impurities. Figure (a) shows the GMR ratio for Co/Cu multilayers with only impurities (\bullet), only vacancies ($+$) and impurities and vacancies together (\diamond). Figures (b) shows the spin asymmetry of the current for the same samples. The layer thicknesses are $t_{\text{Cu}}=8\text{AP}$ and $t_{\text{Co}}=15\text{AP}$.

Material	ϵ_s (eV)	ϵ_d (eV)	$ss\sigma$ (eV)	$dd(\sigma, \pi, \delta)$ (eV)	$sd\sigma$ (eV)	h (eV)
Cu	-7.8	-4.0	-2.7	-0.85	1.1	0.0
Co	-4.6	-2.0	-2.7	-0.85	0.9	1.6

TABLE I. Parameters used in the calculations